ELSEVIER

Ceramics International 30 (2004) 251–255

CERAMICS INTERNATIONAL

www.elsevier.com/locate/ceramint

Characterisation of acid activated montmorillonite clay from Tuulant (Mongolia)

J. Temuujin[a], Ts. Jadambaa[b], G. Burmaa[a], Sh. Erdenechimeg[b], J. Amarsanaa[b], K.J.D. MacKenzie[c,*]

[a]Institute of Chemistry and Chemical Technology, Mongolian Academy of Sciences, Ulaanbaatar 51, Mongolia
[b]Department of Materials Science, Science and Technological University of Mongolia, Ulaanbaatar 46, Mongolia
[c]New Zealand Institute for Industrial Research and Development, PO Box 31-310 Lower Hutt, New Zealand

Received 1 April 2003; received in revised form 14 April 2003; accepted 5 May 2003

Abstract

The characteristics of an acid-leached montmorillonite-containing clay from Tuulant (Mongolia) were studied by XRD, DTA-TG, FTIR and N_2 adsorption techniques. Sample aliquots (2 g) were treated with 50 ml 2 M hydrochloric acid at 80 °C for various times. Leaching caused the surface area of the clay to increase 3-fold to 93.9 m^2/g reflecting the formation in the porous silica product of 3–5 nm micropores and 6–10 nm mesopores, the latter resulting from a delaminated card-house structure rather than from the condensation of the micropores. Differences between the surface area of the present leached samples and those reported for other montmorillonite clays reflect the mineralogical composition of the clay, particularly the presence of non-clay constituents.

Keywords: A. Powders: chemical preparation; B. Porosity; D. Clays; Montmorillonite

1. Introduction

Acid leaching of clay minerals is a useful method for obtaining porous material with possible applications as catalysts, catalyst supports, adsorbents, filters, etc. The most widely used acid-activated clays are the bleaching earths, which are capable of removing colour, odour and other impurities from cooking oils of vegetable and animal origin [1,2]. Acid activation of clay minerals is a process for selectively leaching out part of the starting material by utilizing solubility differences towards the leaching solution. Acid-leached products of clay minerals consist mainly of amorphous silica. However, the chemical composition of the reaction products from the same type of clay minerals can depend on the impurities present. The acid-leached product of montmorillonite clay is generally amorphous silica [3,4], but Gates et al. [1] have reported the leaching products of Australian Miles bentonite to be mainly amorphous silica with quartz, cristobalite and feldspar as impurities. That work suggests that feldspar is more stable to acid attack than montmorillonite, but the porous structure of the product was not determined. It is important to take into account the mineral composition of starting materials from various deposits when developing leaching procedures to produce products with properties tailored to specific applications.

The purpose of the present study was to characterize the products of an acid-leached commercial montmorillonite-containing clay from Tuulant (Mongolia). This clay is used as a source of building material [5], but an understanding the physico-chemical and porous properties of the products of its acid activation could lead to a range of other uses for this deposit.

2. Experimental

The montmorillonite-containing clay from Tuulant, Mongolia was passed through a 2 mm diameter sieve before use. The mineralogical content of the clay, determined by XRD using a Rietveld procedure with α-Al_2O_3 as the internal standard, indicated the presence of 40% montmorillonite (PDF 2-014), 40% amorphous material, 4% cristobalite, 5% anorthoclase feldspar

---

* Corresponding author.
E-mail address: k.mackenzie@irl.cri.nz (K.J.D. MacKenzie).

0272-8842/03/$30.00 © 2003 Elsevier Ltd and Techna S.r.l. All rights reserved.
doi:10.1016/S0272-8842(03)00096-8

(PDF 9-478), 2% calcite (PDF 2-069) and traces of quartz. Our attempts to beneficiate this clay encountered difficulties associated with its slow sedimentation rate. Therefore, in the interests of cost-efficiency in processing, the leaching experiments were carried out on the unpurified whole clay. Thus, although the chemical analysis of the whole clay was determined (Table 1), the structural formula of the montmorillonite component was not calculated.

Two-gram aliquots of the clay were added to 100 ml of 2M HCL held at 80 °C. After leaching for times varying from 0.5 to 12 h the mixture was cooled by the addition of 100 ml cold distilled water. The cooled suspension was filtered off, washed several times with distilled water and dried at 105 °C overnight. The crystalline phases in the samples were determined by XRD (Shimadzu LabX XRD-6100) and the chemical compositions were measured by X-ray fluorescence (Rigaku RIX2000). FTIR spectra were determined using a Shimadzu FTIR 8120 spectrometer, the samples being suspended in KBr discs. The specific surface area was measured at 77 K by the BET method with a Quantachrome Autosorb-1 instrument using nitrogen gas. The pore size distribution was calculated in the radius range from 0.6 to 100 nm by the BJH method using the adsorption isotherm.

3. Results and discussion

3.1. Mineralogical composition

Fig. 1 shows the XRD patterns of raw and leached Tuulant montmorillonite clay. Leaching causes the intensity of the montmorillonite peaks to decrease almost to zero after 6 h. The intensities of the feldspar peaks also decrease, but these are still present in the samples leached for 12 h, indicating that feldspar is more resistant to acid attack than montmorillonite. The halo at about 20–24° 2θ becomes clearer due to amorphous silica remaining from leached montmorillonite phase.

3.2. Chemical composition

Table 1 shows the change of chemical composition and porous properties of the montmorillonite clay as a function of leaching time. The chemical composition data indicate that none of the leached samples is pure silica, consistent with the presence of feldspar in the XRD patterns. Leaching for 1 h removes most of the Ca as expected, since a significant proportion of the Ca is present as the acid-soluble carbonate (calcite). After leaching for 6 h the K^+ and Ca^{2+} content became almost constant, but although the concentrations of Al, Mg and Fe ions continued to decrease, they did not completely disappear. After 12 h leaching the XRD peaks of montmorillonite were no longer present. Montmorillonite normally displays tetrahedral substitution of alumina for silica and octahedral substitution of iron and magnesium for aluminum. In the 2:1 clay minerals, the tetrahedral cations are generally the most resistant to acid attack, followed by the octahedral cations, with the interlayer cations the most vulnerable. On this basis,

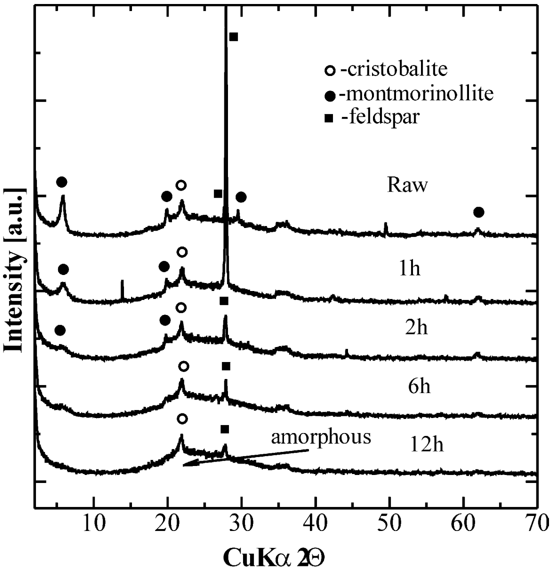

Fig. 1. XRD patterns of starting material and products leached for varying times as indicated.

Table 1
Major oxide composition and porous properties of Tuulant clay and the products of its acid-leaching for varying periods

	(mass%)							S_{BET}[a] (m^2/g)	V_P[b] (ml/g)
	SiO_2	Al_2O_3	MgO	CaO	Fe_2O_3	Na_2O	K_2O		
Unleached	74.3	15.1	3.59	3.32	1.63	1.06	0.95	31.3	0.071
Leached 1 h	77.9	15.05	2.78	0.57	1.36	1.03	1.16	54.2	0.32
Leached 2 h	79.9	13.6	2.49	0.59	1.14	1.04	1.21	67.7	0.11
Leached 6 h	83.7	10.9	1.64	0.49	0.86	1.13	1.25	89.1	0.15
Leached 12 h	88.1	7.72	0.74	0.51	0.65	0.87	1.23	93.9	0.22

[a] BET surface area.

[b] Pore volume.

octahedrally substituted Mg^{2+} and Fe^{3+} substituted in the montmorillonite octahedral layer should be removed at an early stage of leaching; the retention of some Mg and Fe even after leaching for 12 h suggests that they may also be present in the X-ray amorphous phase. XRD of the samples leached for 12 h shows the presence of only a small amount of crystalline cristobalite and feldspar. The significant concentration of Al^{3+}, K^{+} and Na^{+} indicate that these are present in an acid-resistant amorphous phase, or alternatively, they may precipitate as a new X-ray-amorphous phase from the leachate.

3.3. Thermal analysis

The TGDTA curves of montmorillonnite leached for various times are shown in Fig. 2. The thermal analysis curves of the raw clay (not shown here) are typical of montmorillonite [5]. Prolonged leaching causes the dehydration endotherm at about 100 °C to disappear and the weight loss curve to become more gradual. After longer leaching a new broad exotherm appears at about 540 °C, associated with a small weight loss but no change in the XRD pattern (Fig. 1). This thermal effect may therefore be associated with the amorphous precipitate postulated above on the basis of changes in the chemical and mineralogical composition.

3.4. FTIR spectroscopy

Fig. 3 shows the FTIR spectra of the raw and leached samples. The spectrum of the original clay suggests that it contains poorly crystallized components, evidenced by the absorption band at 1090 cm^{-1} and inflexion at 1200 cm^{-1} due to amorphous silica [6], confirming our previous studies of this clay [5]. The raw clay spectrum also contains a broad band at 1430 cm^{-1}, due to the calcite impurity [7]. The IR spectra also suggest that the Al^{3+}, Fe^{3+} and Mg^{2+} ions occupy octahedral sites, since the hydroxyl bending peaks of Al_2OH, AlFeOH and AlMgOH vibrations are present at 915, 881 and 842 cm^{-1} respectively [1,8,9]. An O–H stretching band located around 3620 cm^{-1} has been reported in Mg and Al-enriched dioctahedral smectite [9]. Reported FTIR data for the dioctahedral smectites [8] show a band near 1048 cm^{-1} due to Si–O stretching vibrations of the tetrahedral layer and bands at 518 and 466 cm^{-1} due to Si–O–Al(octahedral) and Si–O–Si bending vibrations respectively. The weak absorption band at 621 cm^{-1} can be identified as the perpendicular vibration of the octahedral cations (R–O–Si) where these are light (R = Al, Mg, Li) and the band at 790 cm^{-1} is attributed to cristobalite.

The FTIR spectra reflect the structural degradation of the clay components and formation of an amorphous silica phase during acid treatment. Leaching causes the intensity of the absorption bands at 3620, 915, 878, 842, 621 and 518 cm^{-1} to decrease, almost disappearing after 12 h reaction. This result reflects the depletion of the octahedral cations (Al^{3+}, Fe^{3+} and Mg^{2+}) from the clay phase. After 12 h leaching, the Si–O stretching bands at 1090 and 1200 cm^{-1} become dominant due to the formation of an amorphous silica phase. However, the persistence of a weak inflexion at 1040 cm^{-1} indicates that the layered structure of the original clay is not fully destroyed. The band at 796 cm^{-1} associated with cristobalite not only survives the leaching process but increases in intensity after 12 h reaction. The presence of

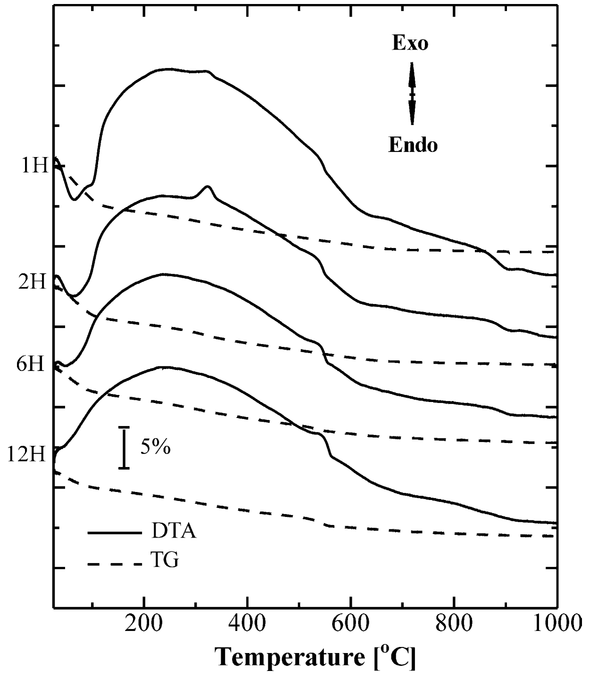

Fig. 2. DTATG curves of samples leached for varying times as indicated.

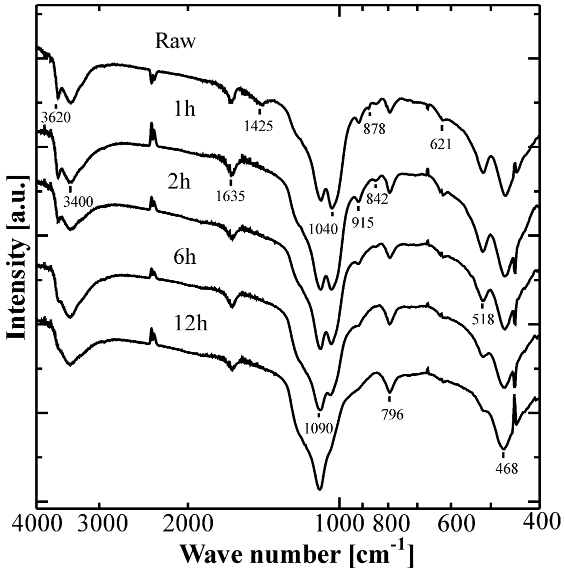

Fig. 3. FTIR spectra of starting material and products leached for varying times as indicated.

a band at about 800 cm^{-1} is usually taken as evidence for a three-dimensional amorphous silica phase [7,9]. The present intensity increase in this region at longer leaching times may suggest that depletion of the octahedral cations is followed by the formation of silica with a three-dimensional cross-linked structure. One interesting feature of the present leached clay is the apparent absence of the Si–OH band at 1050 cm^{-1} found in leached clay minerals such as kaolinite, vermiculite and talc [7,10,11]. All these minerals however contain less impurities than the present clay.

3.5. Porous properties

Table 1 shows that the specific surface area of the sample increases significantly up to 6 h leaching, after which it becomes almost constant. The specific surface area of the present clay is much smaller than previously reported for pure montmorillonite ($\approx$180 m^2/g) [3,12]. This observation reflects the presence of non-layer lattice impurities (principally cristobalite, feldspar and calcite) in the present clay. The high surface areas of leached clays arise from the conversion of the layered structures to porous products. The XRD pattern of the sample leached for 12 h (Fig. 1) shows that the intensities of the feldspar peaks are considerably decreased, but this is not accompanied by an increase in the surface area. This suggests the importance of purifying the clay if a leached product of high surface area is required. The presence of large amount of amorphous constituent in this clay must also be taken into account when considering its leaching behavior. The chemical composition of the leached samples (Table 1) suggests that the cations associated with the amorphous component were not leached out; consequently this phase does not contribute to the porosity. The amorphous component may exist in a glassy state from which the cations were not depleted under the present leaching conditions.

N_2 adsorption–desorption isotherms of the unleached and leached clay samples are shown in Fig. 4. All the isotherms are of similar shape to type II, characteristic of non-porous or macroporous adsorbents. However, the observed hysteresis loop is associated with capillary condensation taking place in mesopores and is therefore assigned as type IV [13]. The increase in adsorbed volumes of the leached samples with leaching time can be explained in terms of increasing numbers of pores in the samples. The adsorption and desorption branches of hysteresis loop of the raw clay and of samples leached for 1 and 2 h are nearly horizontal and parallel over a wide range of P/P_0. This shape of isotherm corresponds to a type H4 loop, indicative of narrow slit-like pores [13]. The hysteresis loop of the isotherm becomes broader with longer leaching times and the loop shape begins to resemble a combination of H1 and H3 loops. This may reflect a change from the laminar structure of the original clay to a delaminated card-house structure as observed for pure montmorillonite [3].

Fig. 5 shows the pore size distributions (PSD) of the samples calculated from the adsorption isotherms. The increase in the height of the PSD curve in the microporous region with increased leaching time indicates increasing numbers of micropores. The sample leached for 6 h contains a broad PSD peak centered at 3 nm,

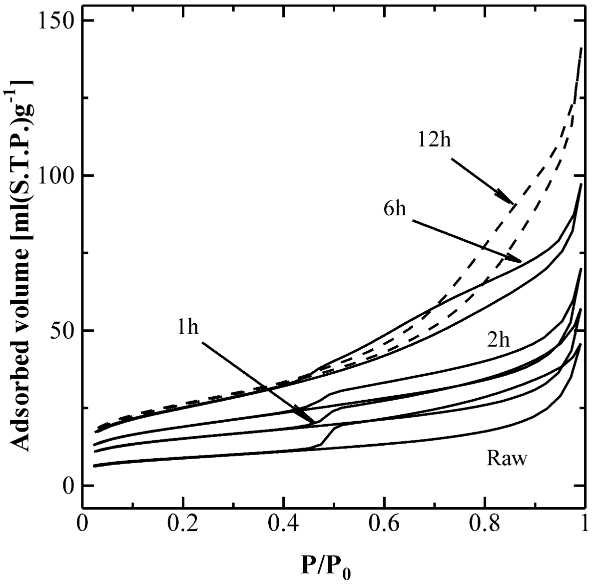

Fig. 4. N_2 adsorption isotherms of the starting material and products leached for varying times as indicated.

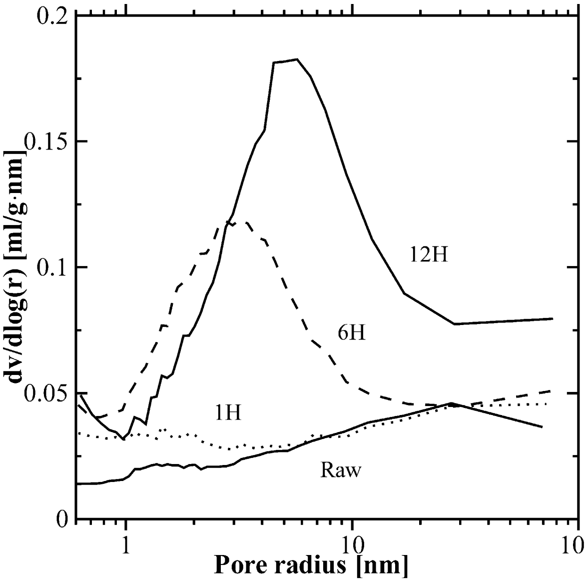

Fig. 5. Pore size distribution curves (PSD) of the starting material and products leached for varying times as indicated, determined from the adsorption branch of the isotherm.

which shifts to 5 nm and increases in height upon further leaching up to 12 h. However, the height of the PSD curve is almost unchanged in the microporous region. Previous work [11] suggests that where mesopores are formed by condensation of adjacent layers of microporous silica, the height of the PSD curve in the microporous region should decrease. The present results suggest that new mesopores appearing between the particles of the amorphous silica form from a card-house structure rather than by condensation of micropores. The PSD indicates that the pores present in the leached samples consist mainly of mesopores of 6–10 nm size. However, the non-clay compounds present in this material make only a small contribution to the porous properties.

4. Conclusions

Montmorillonite-containing clay was treated with hydrochloric acid to prepare surface- active porous materials. The maximum specific surface area achieved was about 94 m^2/g with a pore volume of 0.22 ml/g. The specific surface area of the leached samples is derived from the clay constituent of the starting material, and the presence of non-clay constituents in the original material does not result in an increase in the surface area of the leached products. Mesopores in the leached samples may be formed as a card-house structure between the elementary particles of the amorphous silica.

Acknowledgements

The authors thank The Information Center of Particle Technology, Japan (ICPT) for support under joint project "Utilization of Mongolian raw minerals for preparation of value added material". We are indebted to M.J. Ryan for assistance with the Rietveld XRD analysis.

References

[1] W.P. Gates, J.S. Anderson, M.D. Raven, G.J. Churchman, Mineralogy of a bentonite from Miles, Queensland, Australia and characterization of its acid activation products, Applied Clay Science 20 (2002) 189–197.

[2] H.H. Murray, Traditional and new applications for kaolin, smectite, and palygorskite: a general overview, Applied Clay Science 17 (2000) 207–221.

[3] T. Shinoda, M. Onaka, Y. Izumi, Proposed models of mesopore structures in sulfuric acid-treated montmorillonites and K10, Chemistry Letters (1995) 495–496.

[4] I. Tkac, P. Komadel, D. Muller, Acid-treated montmorillonites—a study by ^{29}Si and ^{27}Al MAS NMR, Clay Minerals 29 (1994) 11–19.

[5] J. Temuujin, Ts. Jadambaa, K.J.D. MacKenzie, Effect of water vapour atmospheres on thermal transformations and mechanical strength of montmorillonite clay compacts, British Ceramic Transactions 99 (N2) (2000) 63–66.

[6] H.H.W. Moenke, Silica, the three-dimensional silicates, borosilicates and beryllium silicates, in: V.C. Farmer (Ed.), The Infrared Spectra of Minerals, Mineralogical Society, London, 1974, pp. 365–382.

[7] J. Temuujin, K. Okada, Ts. Jadambaa, K.J.D. MacKenzie, J. Amarsanaa, Effect of grinding on the preparation of porous material from talc by selective leaching, Journal of Materials Science Letters 21 (2002) 1607–1609.

[8] J. Madejova, J. Bujdak, M. Janek, P. Komadel, Comparative FT-IR study of structural modifications during acid treatment of dioctahedral smectites and hectorite, Spectrochimica Acta A 54 (1998) 1397–1406.

[9] V.C. Farmer, Layer silicates, in: V.C. Farmer (Ed.), The Infrared Spectra of Minerals, Mineralogical Society, London, 1974, pp. 331–363.

[10] J. Temuujin, G. Burmaa, J. Amgalan, K. Okada, Ts. Jadambaa, K.J.D. MacKenzie, Preparation of porous silica from mechanically activated kaolinite, Journal of Porous Materials 8 (2001) 233–238.

[11] J. Temuujin, K. Okada, K.J.D. MacKenzie, Preparation of porous silica from vermiculite by selective leaching, Applied Clay Science 22 (4) (2003) 187–195.

[12] J. Ravichandran, B. Sivasankar, Properties and catalytic activity of acid-modified montmorillonite and vermiculite, Clays and Clay Minerals 45 (1997) 854–858.

[13] K.S.W. Sing, D.H. Everett, R.A.W. Haul, L. Moscou, R.A. Pierotti, J. Rouquerol, T. Siemieniewska, Reporting physisorption data for gas/solid systems with special reference to the determination of surface area and porosity, Pure and Applied Chemistry 57 (1985) 603–619.